Research Square

Preprints are preliminary reports that have not undergone peer review.
They should not be considered conclusive, used to inform clinical practice,
or referenced by the media as validated information.

Unveiling the synergetic effectiveness of PTFE and MWCNTs as additives under steel-steel contact

Anthony Chukwunonso Opia

anthonyopia17@yahoo.com

1) Centre for Research in Advanced Fluid & Processes, Universiti Malaysia Pahang Al-Sultan Abdullah, Pekan, Malaysia

Kumaran Kadirgama

1) Centre for Research in Advanced Fluid & Processes, Universiti Malaysia Pahang Al-Sultan Abdullah, Pekan, Malaysia

Stanley Chinedu Mamah

1) Centre for Research in Advanced Fluid & Processes, Universiti Malaysia Pahang Al-Sultan Abdullah, Pekan, Malaysia

Mohd Fairusham Ghazali

1) Centre for Research in Advanced Fluid & Processes, Universiti Malaysia Pahang Al-Sultan Abdullah, Pekan, Malaysia

Wan Sharuzi wan Harun

3) Faculty of Mechanical Engineering and Automotive Engineering Technology Universiti Malaysia Pahang Al-Sultan Abdullah, Pekan, Malaysia

Augustine Agi

1) Centre for Research in Advanced Fluid & Processes, Universiti Malaysia Pahang Al-Sultan Abdullah, Pekan, Malaysia

Research Article

Keywords: MWCNTs, PTFE, synergistic, lubrication, friction and wear

Posted Date: October 13th, 2026

DOI: https://doi.org/10.21203/rs.3.rs-10956459/v1

License: This work is licensed under a Creative Commons Attribution 4.0 International License.
Read Full License

Additional Declarations: No competing interests reported.

Unveiling the synergetic effectiveness of PTFE and MWCNTs as additives under steel-steel contact

Anthony Chukwunonso Opia[1,2 *], Kumaran Kadirgama[1,2*], Stanley Chinedu Mamah [1], Mohd Fairusham Ghazali[1,3], Wan Sharuzi wan Harun[2], Augustine Agi[1]

[1)] Centre for Research in Advanced Fluid & Processes, Universiti Malaysia Pahang Al-Sultan Abdullah, Pekan, Malaysia.

[2)] Faculty of Mechanical Engineering, Universiti Malaysia Pahang Al-Sultan Abdullah, Pekan, Malaysia

[3)] Faculty of Mechanical Engineering and Automotive Engineering Technology Universiti Malaysia Pahang Al-Sultan Abdullah, Pekan, Malaysia.

Corresponding author E-mail: anthonyopia17@yahoo.com, kumaran@umpsa.edu.my

Abstract

Investigating the tribological performance of multiwalled carbon nanotubes (MWCNTs), polytetrafluoroethylene (PTFE), and MWCNT/PTFE blended as lubricant additives in commercially available base jatropha oil (BJO) during body-body contact was conducted in this work. Using a four-ball tribo tester, the tribological tests were carried out on alloy-steel contacts. To assess the best performance, several concentrations of MWCNT, PTFE, and MWCNTs + PTFE nanomaterials were also varied. The tribological results showed that compared to the BJO, individual MWCNTs, and PTFE, the MWCNTs + PTFE blended nanomaterials in the BJO demonstrated significantly improved friction reduction and higher anti-wear capability. In terms of friction, wear resistance and surface roughness, 1 wt.% MWCNTs (40.08% and 0.33 mm) exhibited outstanding performance wear mitigation while 0.4 wt.% PTFE (49.77 %) produced optimal coefficient of friction. In comparison to the BJO, the BJO with an ideal concentration of 0.8 wt.% MWCNTs + 0.4 wt.% PTFE nanoparticles significantly reduced the wear and friction coefficient by 44.43 % and 55.11 %, respectively. A 3D optical profilometer and a field emission scanning electron microscope were used to analyse the morphology and chemical content of the worn steel substrate surfaces, thus detected elements of the formulations as revealed by energy-dispersive X-ray spectroscopy.

Keywords: MWCNTs, PTFE, synergistic, lubrication, friction and wear

1. Introduction

Due to the lack of effective methods to use chemicals, lubricants, and additives to reduce machine element damage, limit pollutant generation, and improve power from industries and transportation networks, numerous studies have been carried out to reduce excessive friction and wear during equipment mechanisms. According to reports, excessive wear or lubricant film breakdown account for over 50% of severe mechanical failures, and wear is responsible for about 80% of mechanical component failures. These findings highlight the direct impact of tribological performance on operational efficiency and reliability [1], [2]. Therefore, improving rolling bearing lubrication performance, prolonging their service life, and lowering friction-related energy consumption continue to be important scientific and engineering issues in bearing design and real-world applications. In the subject of tribology, however, this is accomplished when the right product is combined with the right tools and work ethic.

The tribological performance of various nanoparticle additions has been extensively studied throughout the years. Certain materials, such as Cu [3], [4], [5], MoS2 [6], [7], BN [8], [9], graphite [10], graphene [11], [12], carbon nanotubes [13], [14], [15], have been demonstrated in lab experiments to reduce wear and friction. The majority of the aforementioned additives have been shown to reduce wear and friction, however others do not. Another well-established and successful approach is the addition of solid lubricants to base oils to improve anti-wear and friction-reduction performance [16]. Numerous studies have demonstrated that a suitable concentration of nano-additives, such as polytetrafluoroethylene (PTFE), can significantly lower the friction coefficient and wear because of their exceptionally low shear strength and superior self-lubricating qualities [17]. According to Liu et al., under water-based lubrication conditions, 0.5 wt.% PTFE@silica Janus nanoparticles considerably decreased wear and friction [18]. Ali et al. showed that the AISI 52100-AISI 1010 tribo-pair's wear and friction performance were significantly enhanced by adding about 1.0 wt.%PTFE nanoparticles to vegetable oil, and that this blend with antioxidant additives produced a synergistic result under high operating conditions [19].

Additionally, a concentration of 3.0 wt.% significantly improved the lubricant's welding load, anti-wear, and friction-reducing capabilities, according to Dubey et al.'s investigation into the tribological behavior of nano-PTFE utilized as a lubricant addition [17]. However, particle agglomeration caused performance to deteriorate with additional concentration increases [17]. PTFE breakdown and its reaction on metal surface to generate a chemically bonded FeF_2 tribo-film were the main causes of the extreme-pressure performance improvement of up to 392% at

an optimal concentration of 6.0 wt.%, according to Saini et al.'s study of the interfacial mechanism and extreme-pressure performance of submicron PTFE particles in bio base oil [20].

Presently, carbon nanoparticles are widely acknowledged as effective additives due to their exceptional physical and chemical properties, including their strong chemical structure, outstanding thermal conductivity, effective load-carrying tendency, and low surface energy [21][22]. Urea-modified fluorinated carbon nanotubes (UF-CNTs) exhibiting hydrophilic properties were synthesized by Min et al. [23]. Urea's amino functionality can efficiently create hydrogen bonds with water in aqueous conditions, giving UF-CNTs better tribological performance and high dispersibility in bio base lubricant. Furthermore, whereas nano additives seem to be perfect for reducing wear and friction, their tendency to group together significantly limits their applicability [23], resulting in poor dispersion and high sticky friction.

The residual charges in an additive's materials cause the H and O atoms to have a significant electric dipole, which grounds them to gravitate toward the charges and instinctively create hydrogen bonds with hydrophilic clusters in an aqueous setting, encasing the nano additives in a hydration layer [24]. This guarantees that the nano additives are separated, giving them superior dispersion and minimal shear force [25], which can be achieved via sonication practices. More so, PTFE polymer chains are commonly utilized in lubrication operation to promote lubricity because of their ability to surround hydrogen atoms by the many functional groups [26]. With friction coefficient of less than 0.026, Zhao et al.'s research polymer grafted hydrogel composite [27] showed a durable low-friction characteristic under very challenging test conditions. Surface functionalization with hydrophilic and charged polymers has been shown to be a dependable technique for enhancing the tribological capability of anti-wear additives.

Understanding Determining the potential applications of different nano additive compounds requires an understanding of their tribopair chemistry. To the best of our knowledge, no comprehensive study has been conducted on the tribological interactions among different MWCNT anti-wear additives and PTFE self-lubricating polymer in jatropha oil and AISI E-52,100 material. The aim of this study was to investigate the tribological lubricity of multi-wall carbon nanotubes (MWCNTs), PTFE polymer, and blended PTFE/MWCNT using jatropha oil as the fundamental lubricant on AISI E-52,100 material. According to the literature [28], these materials were selected because of their effectiveness in basic vegetable lubricants, their eco-friendliness, and their variety of sizes and shapes.

2. Experimental

2.1 Lubricant samples and characterization

The concentrations listed in Table 1 were used to create the oil samples using BJO, MWCNTs, and PTFE additives (supplied by Sigma Arich Malaysia). In this work, 1 wt.% MWCNTs and 0.5 wt.% PTFE were chosen as the concentrations. These concentrations were based on how well they performed in earlier research. Magnetic stirring at 2500 rpm for 1.5 hours was used to prepare the blends; this method worked well for creating homogenous blends. In order to determine the repeatability of the results, the additive composition was chosen to provide a clear and consistent wear and COF decrease within the test conditions in this work, as discovered after three separate experiments.

Table 1. Samples Code and concentrations

Samples Code	Base oil	MWCNT (wt. %)	PTFE (wt. %)
First phase of testing			
BJO	BJO	-	-
BJO + MWCNT	BJO	0.8	-
BJO + MWCNT	BJO	1	-
BJO + MWCNT	BJO	1.2	-
BJO + PTFE	BJO	-	0.2
BJO + PTFE	BJO	-	0.4
BJO + PTFE	BJO	-	0.6
Second phase of testing			
BJO (A)	BJO		
1.2 wt.% MWCNT + 0.2 wt.% PTFE (B)	BJO	1.2 wt.% MWCNT	0.2 wt.% PTFE
1.2 wt.% MWCNT + 0.4 wt.% PTFE (I)	BJO	1.2 wt.% MWCNT	0.4 wt.% PTFE
1.2 wt.% MWCNT + 0.6 wt.% PTFE (D)	BJO	1.2 wt.% MWCNT	0.6 wt.% PTFE
1 wt.% MWCNT + 0.2 wt.% PTFE (J)	BJO	1 wt.% MWCNT	0.2 wt.% PTFE
1 wt.% MWCNT + 0.4 wt.% PTFE (F)	BJO	1 wt.% MWCNT	0.4 wt.% PTFE
1 wt.% MWCNT + 0.6 wt.% PTFE (C)	BJO	1 wt.% MWCNT	0.6 wt.% PTFE
0.8 wt.% MWCNT + 0.2 wt.% PTFE (E)	BJO	0 wt.% MWCNT	0.2 wt.% PTFE
0.8 wt.% MWCNT + 0.4 wt.% PTFE (G)	BJO	0 wt.% MWCNT	0.4 wt.% PTFE
0.8 wt.% MWCNT + 0.6 wt.% PTFE (H)	BJO	0 wt.% MWCNT	0.6 wt.% PTFE

.

2.2 Analytical tools

A field emission scanning electron microscope (FESEM, JEOL-6100, JOEL Co., Japan) equipped with energy dispersive X-ray spectroscopy (EDS) at a magnification of 200 nm was used to examine the morphology and elemental components of MWCNT, PTFE and MWCNT-PTFE hybrid. Concurrently, the polyphosphate surface structure was investigated. A dynamic light scattering (DLS) particle size machine was used to measure the particle size distribution. Chemical bonding signals were obtained using Fourier transform infrared spectroscopy (FT-IR). The Raman spectrometer operated in the 400–2500 cm^{-1} spectral range and employed line scan mode to detect the carbon signals. Using the thermal gravimetric analysis (TGA) equipment, the thermal characteristics were measured between 50 and 950 ^{o}C at a heating rate of 10 ^{o}C per minute under nitrogen.

2.3 Rheological characterization

A rotational rheometer (Anton Paar MCR702e Multidrive) with a rheological cell attached to a concentric cylinder flow geometry (DG28.91) was used to measure the shear viscosity of the oil samples. This can have an impact on the viscosity of oils and, consequently, the tribological performance.

2.4 Tribological testing

Tribological assessments of the oils were performed using a four-ball tester (Fig. 1) in agreement with the test parameters listed in Tab. 2. According to the approach described by [29][30], the test circumstances were based on the standard ASTM D4172 protocol. The four-ball tester was equipped with a direct current (DC) power supply to supply constant voltage through the four-ball connections. The standard AISI 52100 bearing steel balls that were tested had a diameter of 12.7 mm, a surface roughness of 0.02 μm, and a hardness of 64 HRC. The tester's software measured and recorded CoF for post-analysis. The wear scar diameter for each test was calculated by measuring the circular-type wear scars that developed on the three bottom balls using optical microscopy. To generate the composition of the tribofilm generated, a circular wear scar from one of the three bottom balls and a ring-type scar from the upper ball used for each test were also investigated using energy-dispersive X-ray spectroscopy (EDS) using a Jeol SEM microscope. After testing, an atomic force microscope (AFM) is used to evaluate the wear scar volume and depth on the flat plate.

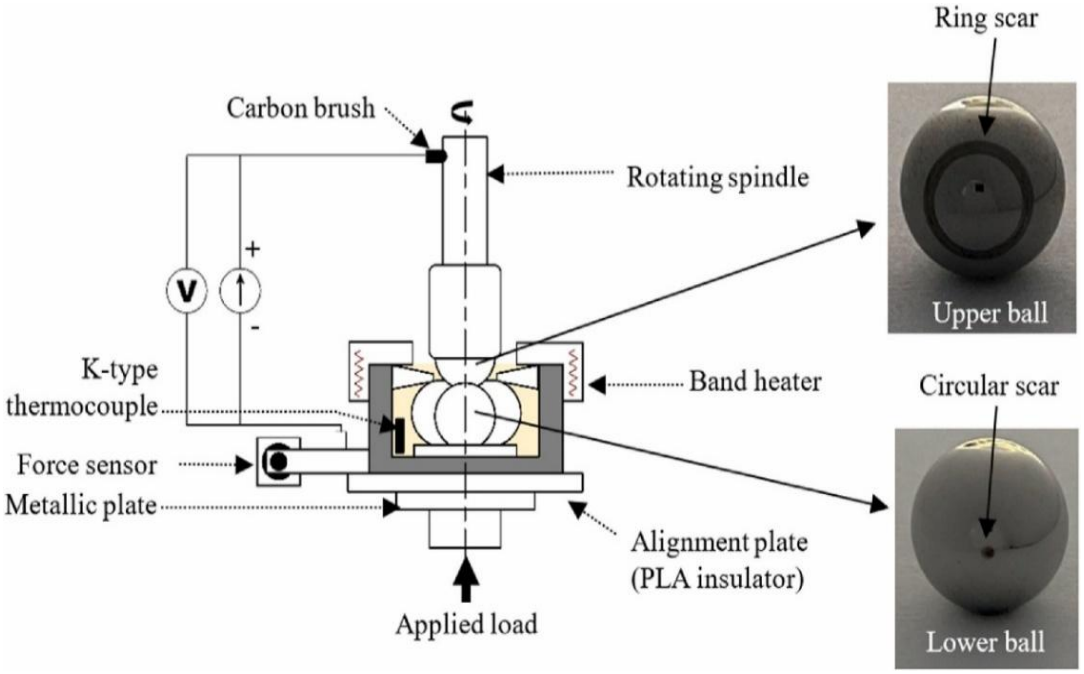


Fig. 1. Presentation of four-ball test set-up and snapshots of the upper and lower balls.

Tab. 2. Analysis operating conditions.

s/n	Parameter	Value
1	Test duration [minutes]	60
2	Load Kg	40, 60, 80, 100, 120
3	Humidity [%]	32
4	Amount of oil [ml]	25
5	Speed [rpm]	80, 100, 1200
6	Temperature [°C]	75±2
7	Voltage range [V]	0.6-1.6
8	Maximum Hertzian contact pressure [GPa]	4.5
9	Number of each test (new sample and new balls)	3

3. Results and discussion

3.1 Characterization findings

Fig. 3a–c displays micrographs taken with a FESEM for both pure and mixed nanoparticles. The spherical and amorphous morphology of dry PTFE nanoparticles, which appear to cluster due to their plymer nature, is depicted in Fig. 3a. A microscopic image of MWCNT nanoparticles showed tube like structure nano-sized tubes as seen in Fig. 3b due to the lack of constraint in the direction of thickness. Spherical PTFE nanoparticles are clearly well trapped within the carbon nanotubes in Fig. 3c, which shows a picture of a homogeneous combination of PTFE and MWCNT nanoparticles. However, the detected elements were presented in Tab. 3.

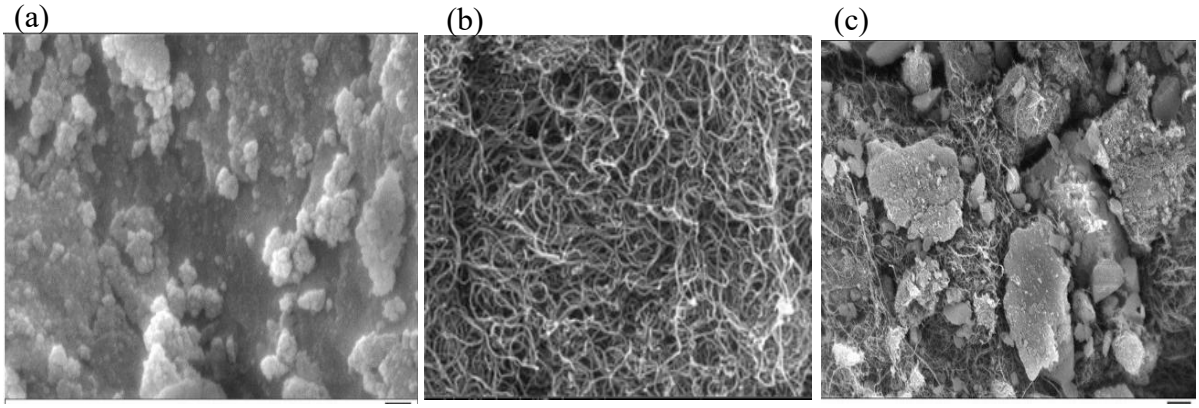


Fig. 2: FESEM images of nano additives of (a) PTFE, (b) MWCNT and (c) MWCNT/PTFE

Tab. 3 Elemental distribution in MWCNTs and PTFE under EDS analysis

Material/Elements (wt.%)	C	O	P	F
MWCNTs	80	20	-	-
PTFE polymer	11.8	8.5	42.3	37.8
MWCNT-PTFE	51.61	12.01	21.1	18.77

The Raman spectroscopy analysis of MWCNT is shown in Fig. 3 (a). It shows two peaks at 1245.70 cm^{-1} and 1580.31 cm^{-1}, respectively. The record on the peaks were ascribed to the vibrations of the carbon atoms in the graphene layer. The results matched the findings that had been reported [31]. The G-band's band defect is more noticeable than the D-band's intensity.

FT-IR was used to assess the functional groups in the formulation as shown in Fig. 3 (b). Due to functional groups, every other portion of the curve, with the exception of the base PTFE polymer's ending curve, resembles the blended additives. The samples' spectra reveal functional group distortion bands for methyl and methylene CH_3 and CH_2 at 1685.11 cm^{-1} and 1492 cm^{-1}, as well as aliphatic broadening bands CH_3 and CH_2 at 2887.33 cm^{-1} and 2795.66 cm^{-1}. An enormous and prevailing band at about 3355.09 cm^{-1} was initiate in the PTFE when comparing the behaviours and functional groups in the spectra of the various samples. However, this band was reduced under the spectra of blended samples due to the lower amount of O–H/N–H group, which resulted in shrinkage on the peaks, particularly when MWCNTs were added. The hydroxyl group (OH) was shown to be linked to a rocking vibration in the PTFE spectra at the 3718.21 cm^{-1} band, which was inadequate for other samples and caused in peak shift.

This is due to the fact that the propagation of oil monomer components inside the polymer chains had a slight structural variation at room temperature and in the absence of

external influence [31]. However, every other sample exhibited a significant change, which was explained by the identification of different molecular components and a reduction in the C=C group caused by the addition of base lubricants. The high vibration of the N–H group and its shared vibration with the C–H group led to the development of peaks at 1338.50 cm^{-1} and 997.51 cm^{-1} when MWCNT + PTFE was utilized; nevertheless, other samples displayed strong shifts indicating the production of new bound in varied unique formulations. The generated spectra from those samples and those of previously discovered peaks that are comparable to each other confirmed the compatibility of MWCNTs, PTFE, and base oil lubricant. The results were in line with previous research [32].

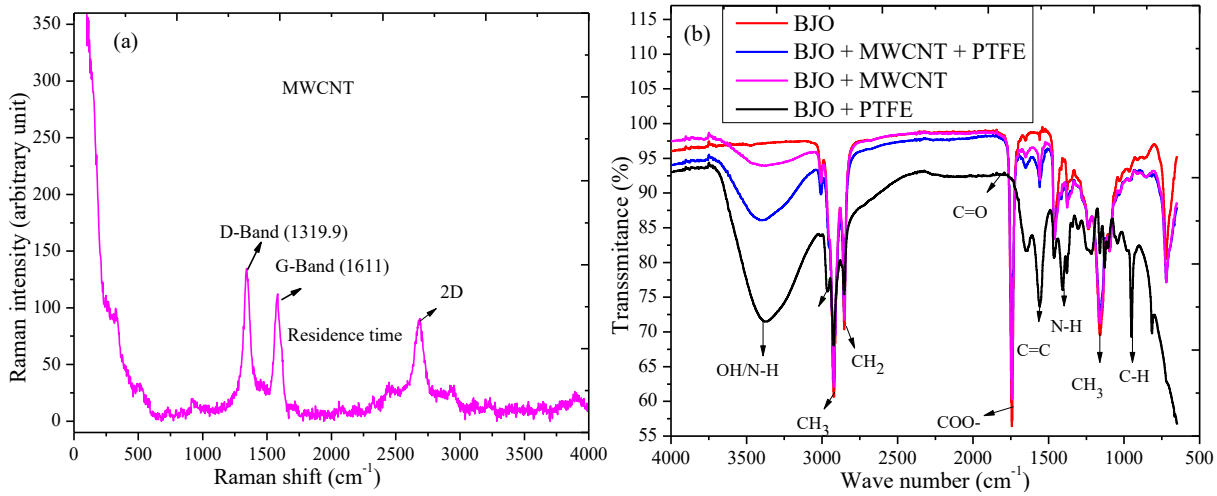


Fig. 3. (a) Raman spectroscopy of MWCNT and (b) FT-IR of the various samples.

The effectiveness PTFE, MWCNT, and PTFE-MWCNT on retaining heat was assessed by TGA analysis, as shown in Fig. 4 (a). This is done to ascertain how resistant additives are to heat when added to lubricants. The analysis of the basic lubricant alone revealed a weight drop of 52.7%. As observed, the weight loss was significantly decreased when paired with different additives, falling to 49.2%, 44.2%, and 32.9% under PTFE, MWCNTs, and PTFE-MWCNT, respectively. The drop demonstrates that, in comparison to base lubrication, the embedding of additives positively reduced the temperature effect on the created lubricants; nevertheless, this effect was more noticeable under PTFE and MWCNT. The PTFE, MWCNT, and PTFE-MWCNT trends were similar, indicating strong compatibility that led to enhanced thermal characteristics. Bhadra made a similar observation on their analysis [40]. Fig. 4 displays the distribution particles of the additives MWCNTs and PTFE-MWCNT under a dynamic light scattering (DLS) particle size machine. The findings demonstrate that the chosen PTFE, MWCNT, and PTFE-MWCNT polymer additives effectively disperse ethanol via sonication, with average mean particle sizes of 37.9 nm, 17.5 nm, and 48.3 nm, respectively.

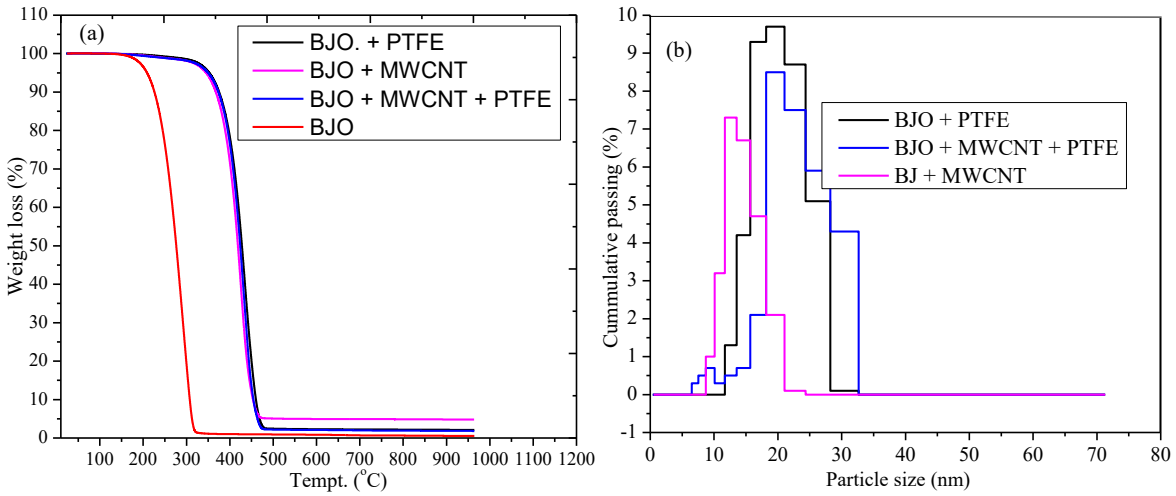


Fig. 4. (a) TGA and (b) dynamic light scattering of the samples used.

The of BJO, blended PTFE, MWCNTs, and PTFE-MWCNT additives at various concentrations and temperatures between 40 and 100 °C are displayed in Fig. 5, and the related viscosity index is shown in Fig. 5 (a). The graphic demonstrates how each tested lubricant's kinematic viscosity decreases as temperatures rise. This is comparable to documented literature [41, 42]. At 40 °C and 100 °C, BJO produced 27.4 cSt and 7.5 cS t, respectively. The blended lubricant progressively loses its viscometric qualities at high temperatures, exhibiting lower values due to the thermal impact [39]. Additionally, results showed that all oils, the exception of 0.6 wt.% PTFE, had viscosity amounts that were closer to one another at 100 degrees Celsius when additives were added. However, 0.4 wt.% + 1 wt.% MWCNT showed rather distinct results, indicating moderate viscosity in the solution.

Due to the absence of polymer ingredients, MWCNT additives exhibit weak viscosity tendency, which is comparable to the performance of 0.4 wt.% PTFE. The optimal viscosity value was 38.4 at 40 °C for 0.6 % PTFE, 18.2 cSt at 100 °C, and 35.7 cSt at 40 °C and 14.9 cSt at 100 °C for 0.4 wt.% PTFE, in contrast to BJO at 27.5 cSt and 8.1 at 40 and 100 °C. BJO produced a viscosity index of 210.3 when the viscosity index was evaluated as shown in Fig. 5 (b). Under 0.4 wt.% PTFE + 1 wt.% MWCNT had the highest value (427.3), followed by 0. 6 wt.% PTFE (420.9), according to the study. As seen in Fig.6 (b), 0.8 wt.% MWCNT (390.7) had the lowest viscosity index of any nano lubricant. This shown that the concentration cannot produce adequate lubrication and that the high concentration may be incompatible. Similar findings have been documented [43].

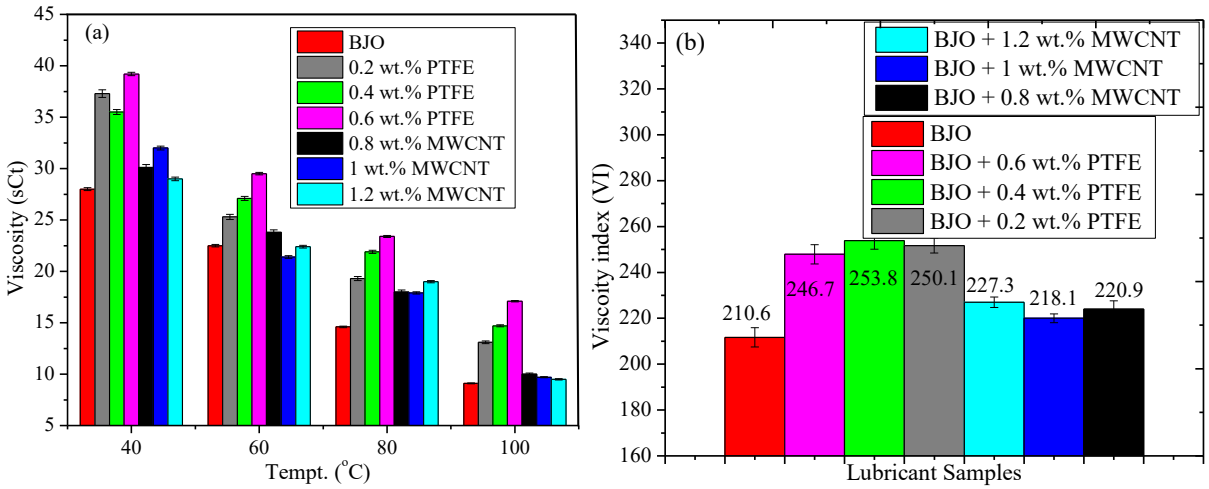


Fig. 5. Analysis of (a) viscosity against temperatures and (b) viscosity index as used in the study

3.2 Frictional Analysis

The coefficient (COF), surface roughness (Ra) and wear diameter (WSD) of each additive sample was tested under 80 N and further investigated at other different loads (40, 60 and 100 N) at different operating speeds as displayed in Fig. 6 in comparison to pure BJO. lubricant. As revealed in Fig. 6 (a), all samples showcase a good COF reduction compared BJO. As demonstrated in Fig. 6 (a), the average COF of base lubricant alone under 80 kg was 0.217. In relation to that, MWCNT concentrations of 1.2 wt.%, 1 wt.%, and 0.8 wt.%, yielded COF reduction of 44.2%, 45.2% and 37.8% whereas PFTE concentrations of 0.6 wt.%, 0.4 wt.%, 0.2 wt.% as mention in lubrication formulation (Tab. 1) produced COF reduction of 48.8%, 49.8% and 46.1%, respectively. The study observed that PTFE had a bigger effect than MWCNTs, with COF ranges from 0.109 to 0.117, while MWCNTs range from 0.119 to 0.135. As presented in Fig. 6 (b), under surface roughness assessment, inclusion of additives reveals wear reduction, thus demonstrated the MWCNT performed better the PTFE. Because of their special tubular nanostructure, remarkable mechanical strength, and capacity to create protective tribofilms during sliding, MWCNTs exhibit great wear-resistant performance. However, 1 wt.% MWCNT produced the optimal results followed by 1.2 wt.% MWCNT before 0.8 wt.% MWCNT, while PTFE candidates yielded very similar and close related values indicating poor anti wear tendency.

To better understand behaviour under the testing setups, the friction reduction and anti-wear impacts of the selected additives compared to BJO were examined at various loads at an operating speed of 1000 rpm, as illustrated in Fig. 6 (c and d). The average friction coefficient and ball wear scar diameter fell more significantly in comparison to the base lubricant as the loads increased from 40 kg to 80 kg, but increased at 100 kg. This is due to the fact that

nanoparticles' diffusion into the contact area aids in the creation of tribofilms [26]. At 40 kg, 60 kg, 80 kg and 100 kg under BJO the friction coefficient and wear diameter were 0.137 and 0.527, 0.185 and 0.543, 0.217 and 0.571, 0.219 and 0.583, respectively. Using MWCNT, the COF varies from 0.117 to 0.161, while PTFE yielded range from 0.109 to 0.121, respectively. Accordingly, the study discovered that optimal COF reduction was under 0.4 wt.% PTFE, while best of wear reduction was observed with 1 wt.% MWCNT. Thus, all PTFE candidates demonstrates better COF performance while MWCNT yielded outstanding wear protection. The percentage COF and WSD reduction generated from the use of various formulation are presented in Tab. 4, depending on the imposed load.

Tab. 4. % reduction in worn scar diameter and COF from individual additions

Lubricants/condition	Average COF reduction (%)				Average WSD reduction (%)			
	40 N	60 N	80 N	100 N	40 N	60 N	80 N	100 N
Base jatropha oil	0.137	0.185	0.217	0.219	0.527	0.543	0.571	0.583
0.8 wt.% MWCNTs	8.76%	26.89%	23.82%	23.33%	23.91%	28.11%	37.79%	31.05%
1 wt.% MWCNTs	10.94%	31.31%	38.53%	31.22%	25.80%	34.59%	46.08%	42.92%
1.2 wt.% MWCNTs	5.84%	26.89%	24.34%	24.36%	22.01%	36.22%	44.24%	41.55%
0.2 wt.% PTFE	13.87%	37.84%	46.08%	44.75%	8.35%	8.10%	10.16%	12.35%
0.4 wt.% PTFE	15.33%	42.16%	49.77%	48.97%	24.29%	23.94%	22.42%	19.21%
0.6 wt.% PTFE	12.41%	38.38%	48.84%	46.12%	10.06%	8.47%	12.25%	13.04%

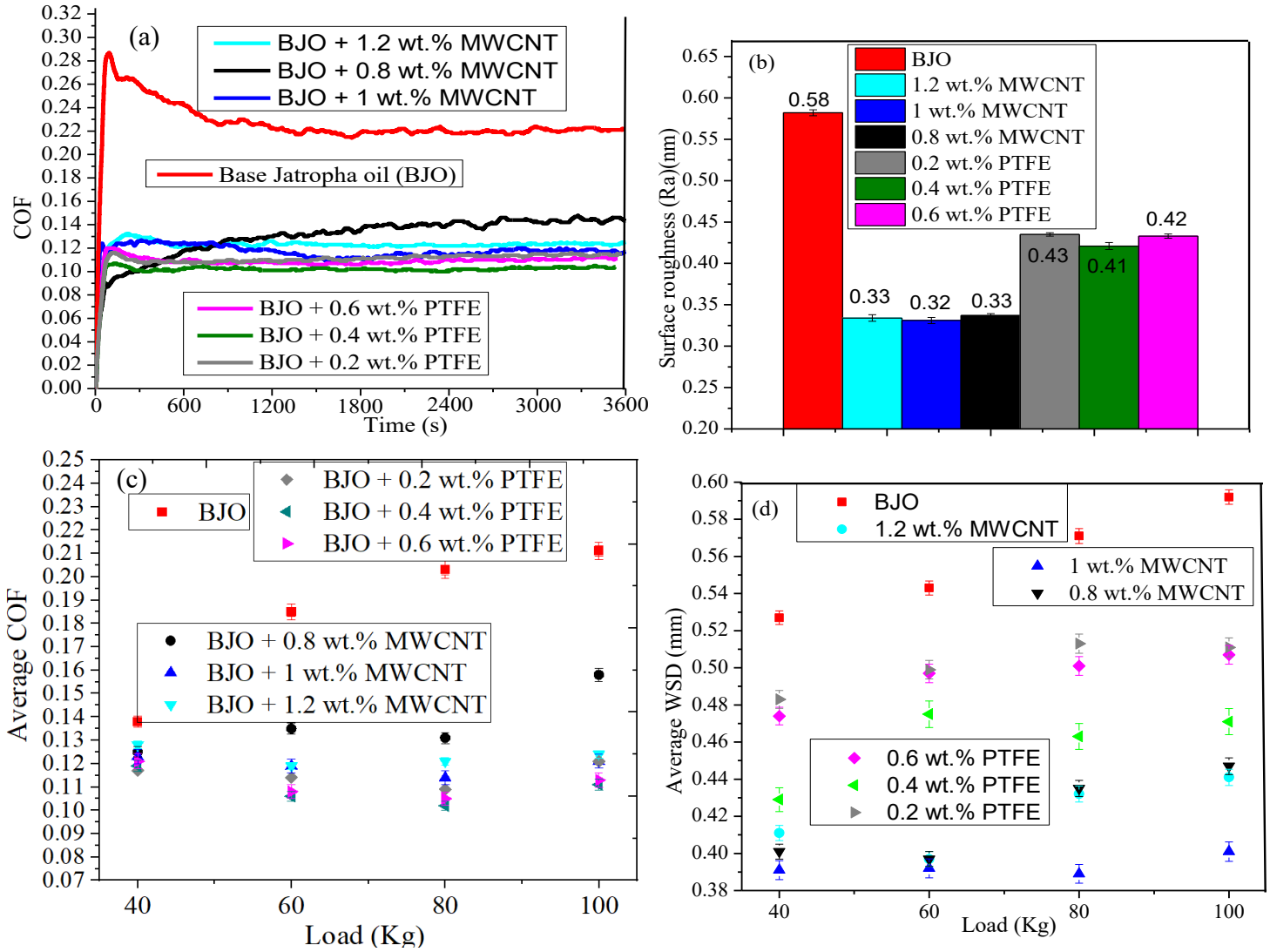


Fig. 6. (a) Coefficient of friction, (b) surface roughness (Ra), average COF and average WSD from the various individual additives under different loads; 40 N, 60 N, 80 N and 100 N, and temperature of 75°C.

To further assess industrial applicability, it is necessary to combine the two separate additions to examine their synergistic effect because the performance of the individual additives varied. The synergistic tendency of MWCNT and PTFE and tribological performance was evaluated under extended operating condition (80 kg, 100 kg and 120 kg) and elevated temperature (80 °C) with rotation speed of 1200 rmp, as shown in Fig. 7. The findings show that BJO undergoes pronounced COF fluctuations (Fig. 7 (a)) and severe wear loss (Fig. 7 (b)) during prolonged testing. The BJO graph shows irregular trend throughout the time duration. This indicates gradual breakdown of the lubricating film under cumulative fatigue. The BJO produced COF value of 0.568 under 100 kg. In contrast, the various formulated MWCNT + PTFE system remains highly stable and enhanced in all the tested samples, thus revealed synergistic tendency with 0.8 wt.% MWCNT + 0.4 wt.% PTFE (G) (COF = 0.341) showing optimal frictional control. Accordingly, the surface roughness (Ra) was examined via microscopy using a surface profilometer. The findings showed that the blending samples revealed outstanding performance compared to individual additives tested, supported the findings under COF analysis (Fig. 6 (a and b)).

Again, as shown in Fig. 6 (c and d), the various blended samples were tested under different loads in terms of COF and WSD. Corresponding to the previous findings, the application of 0.8 wt.% MWCNT + 0.4 wt.% PTFE demonstrated remarkably good reduction in both COF and wear reduction, while other samples revealed their friction controls in different degree. The study observed that during the testing, the diminished viscosity of the various formulation typically triggers elastohydrodynamic lubrication (EHL) film collapse, transitioning to severe boundary lubrication but more pronounced with BJO. Nonetheless, under 100 kg, 0.8 wt.% MWCNT + 0.4 wt.% PTFE (G) provides sufficient protection in this higher working condition, lowering COF, Ra, average COF and average WSD by 57.01% and 37.61%, respectively. The enhanced thermal stability suggested by the TGA measurements is consistent with this behaviour. This synergistic reinforcement shows that MWCNT + PTFE significantly increases the BJO's load-bearing capacity, guaranteeing dependability under heavily stressed regimes. The operation produced higher frictional energy and amply illustrated the development of better tribo-film due to the elevated operating conditions. However, this could be because of the superior sacrificial layer brought about by favourable tribo-chemistry and frictional energy between the molecular components of the lubricant and the substrate. As reported [33], [34] similar findings regarding the behaviour of microparticles in olive oil under boundary and mixed lubricating conditions.

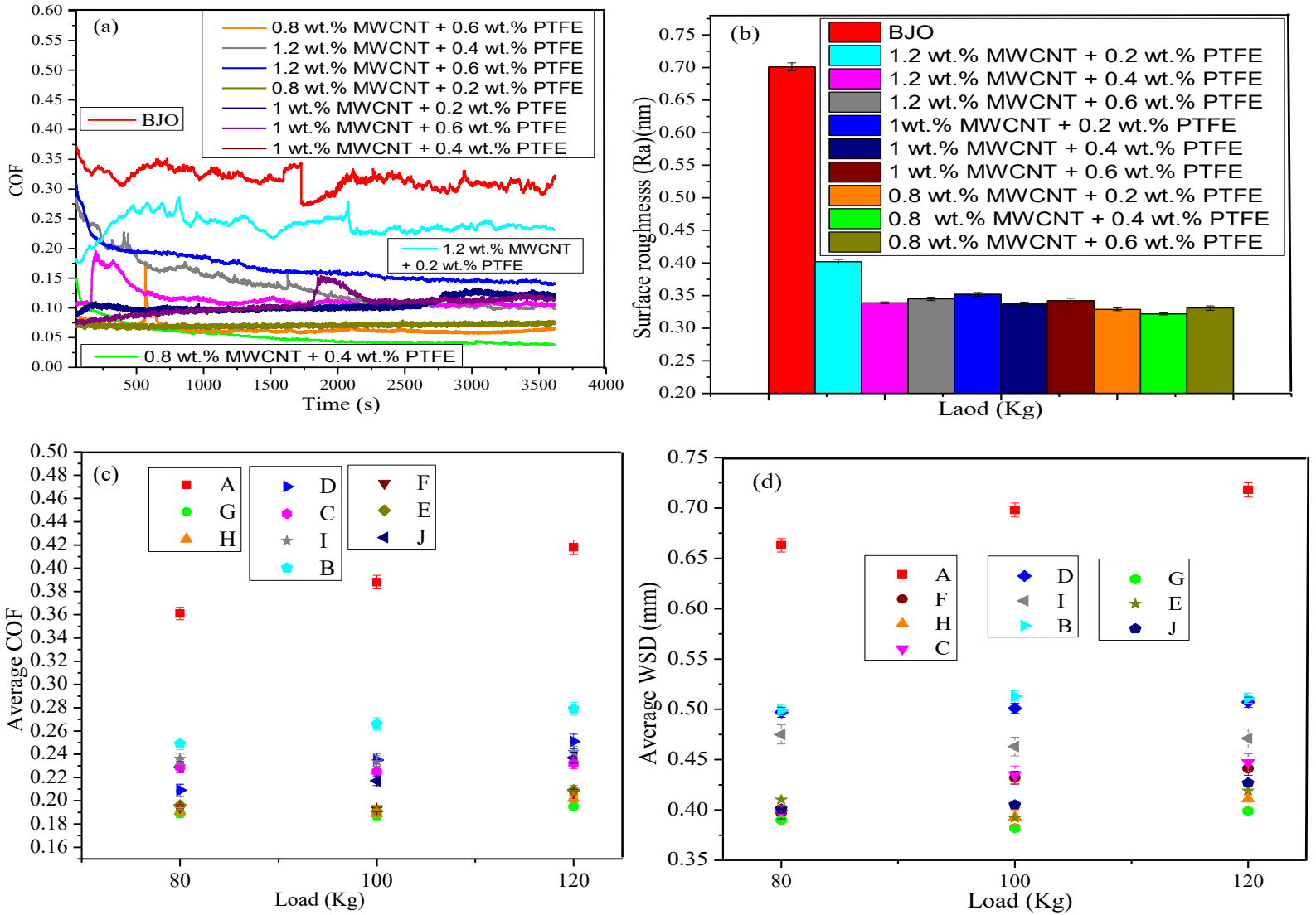


Fig. 7. (a) Coefficient of friction, (b) surface roughness (Ra), average COF and average WSD from the various blended concentrations additives under different loads; 80 Kg, 100 kg and 120 Kg, and temperature of 80°C

From the various investigation analysis, Tab. 5 lists the different COF and wear control from various mixed nano lubricants.

Tab. 5. COF and Ra values recorded from different lubricants

Lubricants/ Condition (Code)	Average COF reduction (%)			Average WSD reduction (%)		
	@ 80 kg	@ 100 kg	@ 120 kg	@ 80 kg	@ 100 kg	@ 120 kg
BJO (A)	0.363	0.382	0.421	0.663	0.693	0.718
B	32.51%	31.68%	35.63%	24.73%	25.97%	28.83%
C	35.81%	38.22%	42.76%	25.04%	27.71%	29.39%
D	36.36%	40.05%	42.04%	28.96%	33.19%	33.84%
E	39.94%	42.15%	43.71%	40.12%	37.23%	37.74%
F	42.98%	44.76%	48.93%	40.42%	37.66%	38.58%
G	48.21%	55.11%	52.09%	41.18%	44.43%	44.16%
H	46.28%	50.00%	51.78%	39.52%	41.56%	40.53%
I	36.36%	44.76%	42.99%	40.87%	43.27%	42.76%
J	39.12%	45.29%	45.61%	38.16%	43.43%	41.64%

Note: BJO = A; 1.2 wt.% MWCNT + 0.2 wt.% PTFE = B; 1 wt.% MWCNT + 0.6 wt.% PTFE = C; 1.2 wt.% MWCNT + 0.6 wt.% PTFE = D; 0.8 wt.% MWCNT + 0.2 wt.% PTFE = E; 1 wt.% MWCNT + 0.4 wt.% PTFE = F; 0.8 wt.% MWCNT + 0.4 wt.% PTFE = G; 0.8 wt.% MWCNT + 0.6 wt.% PTFE = H; 1.2 wt.% MWCNT + 0.4 wt.% PTFE = I; 1 wt.% MWCNT + 0.2 wt.% PTFE = J; as used in the study.

Furthermore, as to ascertain the efficacy of the formulation lubricity, as shown in Fig. 8, the COF, Ra, WSD and wear rate of the optimal concentration (0.8 wt.% MWCNT + 0.4 wt.% PTFE) were examined in comparison to the BJO under loads of 100 Kg at operating speed of 1500 rpm. When compared to the results under 100 Kg (Fig. 8(a)), the study revealed that the COF decreased significantly when compared to BJO lubricant, indicating that the use of 0.8 wt% MWCNT + 0.4 wt% PTFE is very effective as depicted in Fig. 8 (a and b). At 100 Kg, BJO lubricant produced COF of 0.0905 and Ra of 0.74, whereas 0.8 wt.% MWCNT + 0.4 wt.% PTFE produced COF of 0.0711 and Ra of 0.33.

Applying 0.8 wt.% MWCNT + 0.4 wt.% PTFE significantly reduced the study's average COF and WSD analysis, as seen in Fig. 8 (c and d), when compared to BJO. The WSD and wear rate of BJO under 120 Kg was 0.63 mm and 11.7 * 10^{-3} mm^3/N.m, this produced a WSD percentage reduction of 50.7% and 56.4, respectively for 0.8 wt% MWCNT + 0.4 wt% PTFE. The findings demonstrate effective surface protections of 0.8 wt% MWCNT + 0.4 wt% PTFE in comparison to BJO. It was discovered that the operation could generate the frictional energy required for successful tribo-reactions with tribo-film formations at 1500 rpm, which reduced wear and friction. This outcome was consistent with reports found in the literature [35].

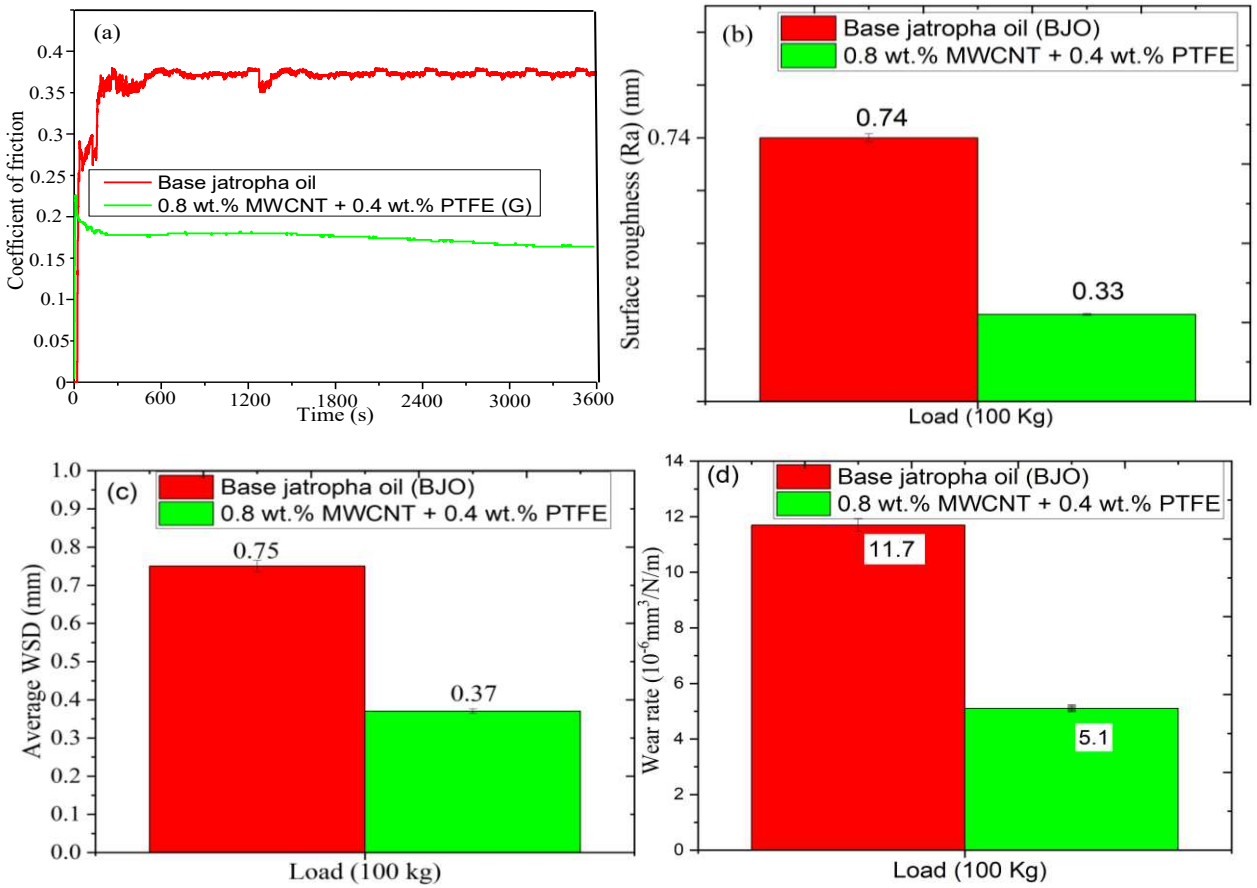


Fig. 8. (a) Coefficient of friction; (b) surface roughness (Ra); (c) average WSD and (d) wear rate from the optimized additives 0.8 wt.% MWCNT + 0.4 wt.% PTFE compared to BJO (Under 100 kg, 75 °C, 1500 rpm)

3.3 Wear scar micrographs and additive mechanism

In comparison to BJO, the surface lubricated with 0.8 wt.% MWCNT + 0.4 wt.% PTFE seems smoother and shallower as depicts in Fig. 9. The tribo-chemistry between the MWCNT and PTFE on the sliding surface caused some healing effects on the grooves. The wear-resistant potential of the nanoparticles and additional EDS inspection are indicated by the red lines (Figs. 9 (a1-b1) on the lubricated surface. By using EDS to reveal elements distribution on the different lubricated surfaces, as indicated in Tab. 6, the anti-wear property improvement from MWCNT + PTFE particles was also demonstrated. This clearly demonstrates that MWCNT + PTFE particles implanted on the contact surfaces create a tribo-film that reduces wear and friction. This outcome is comparable to the earlier analysis of nanoparticles on steel contacts [16][36], [37].

Fig. 9 (c and d) displays the 3D topographical pictures of the lubricated surfaces along with the wear depth (Wd) that corresponds to them. The wear volume and surface roughness were greatly decreased by the addition of MWCNT + PTFE particles. The rolling motion toward surface separation may be the source of this. Additionally, the superior performance of MWCNT + PTFE is ascribed to

its nanoscale, which diffuses into the worn valleys and friction zone and helps the sliding surfaces create an efficient tribo-film during tribo-chemistry operation. The literature has suggested a number of ways that nanoparticles in nanofluid can reduce wear and friction, including the rolling effect, mending/healing effect, improved thermal stability, polishing, and viscosity alteration performance.

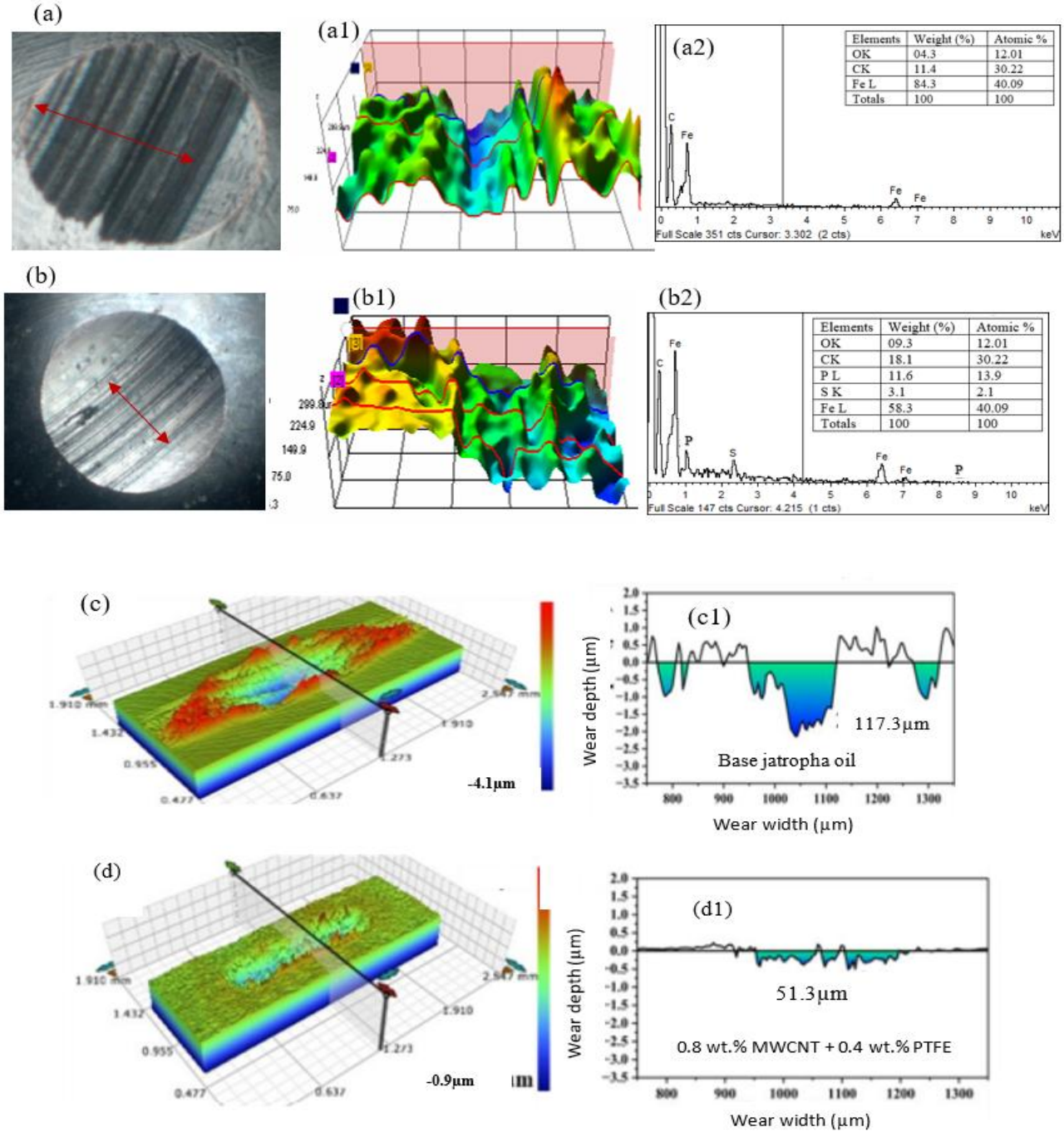


Fig. 9: (a and b) SEM, 3D image showing the Ra and the corresponding EDS; (c and d) 3D images showing wear scar and the corresponding wear depth under different working operations.

The EDS analysis of the different samples is shown in Tab. 6. As observed, Fe and Cr were found to be significantly higher under BJO lubricated surface but to be lower when additives (MWCNT + PTFE) were applied. Similar to a prior work [38], [39], the presence of F, P, N, and a large amount of C on MWCNT + PTFE under EDS assessment indicated that the particles were involved in the tribological process and hence had important anti-wear and friction-reducing activities during lubrication.

Tab. 6. EDS elemental distributions analysis on the lubricated surfaces

Components	C	Cu	O	Cr	Fe	N	F	P
BJO	8.11	-	8.90	3.53	81.50	-	-	-
MWCNTs	16.71	-	9.8	1.02	64.1	-	11	5

This study found no evidence of a polishing impact from the nanofluid lubrication based on the wear performance and friction of the nanoparticle (MWCNT + PTFE). Fig. 10 models the rolling action and healing mechanism of the nanoparticle (in this case, MWCNT + PTFE). This is due to the fact that MWCNT + PTFE elements were present on every surface that the MWCNT + PTFE nanofluid lubricated, which lowers the value of the Fe element in steel. Thus, the primary functions of MWCNT + PTFE during lubrication are rolling and mending/healing. However, as Fig. 10 (b) illustrates, the nanoparticles' rolling mechanism reduced wear during sliding by keeping the two bodies apart from direct contact. The decrease in the size of the furrows seen on the surfaces lubricated with the MWCNT + PTFE addition corroborated the outcome. Furthermore, the substrates demonstrated wear healing as a result of the MWCNT particles filling the troughs during lubrication. The following is a suggested tribological improvement from MWCNT + PTFE lubrication:

Equations (1) and (2) of the Hamrock-Dowson equation for elastic lubrication [40] [41] can be used to estimate the observed minimum film thickness hmin. where η is dynamic viscosity, R is the balls' radius (12/2 = 6 mm), Wy is the applied load, Ue is the operating speed, and Vball and Eball are the steel ball's elastic modulus and Poisson's ratio (AISI 52100). applying the proper values and using 0.8 wt.% MWCNT + 0.4 wt.% PTFE for the analysis. For 100 kg, the lubricant's computed film thickness at various contacts was 33 nm.

$$h_{min} = 2.8\mathrm{R}\ \left(\frac{\eta u_e}{ER}\right)^{0.65}\ \left(\frac{\mathrm{W}_y}{ER^2}\right)^{-0.21} \quad (1)$$

$$\frac{1}{E} = \frac{1}{2}\left(\frac{1-V_{ball^2}}{E_{ball}(up)} + \frac{1-V_{ball^2}}{E_{ball}(down)}\right) \quad (2)$$

Due to heat from friction and increased contact pressure can lead to a potential tribo-chemical response among additives and their surroundings, metal surfaces are crucial in the interface amid nano additives and lubricant molecules in body-body sliding lubrication [11], [42], [43]. As a result, on the friction surface, a tribofilm may develop. In this instance, MWCNT-PTFE, the lubricant, and their chemically bound components produce the tribofilm adsorption. The tribofilm mechanism is frequently the most comprehensive model for describing the anti-wear and friction reduction properties of nanolubricants (Fig. 10). The majority of studies attributed nanolubricants' superior lubrication effectiveness to their ability to produce a protective coating over rubbing surfaces.

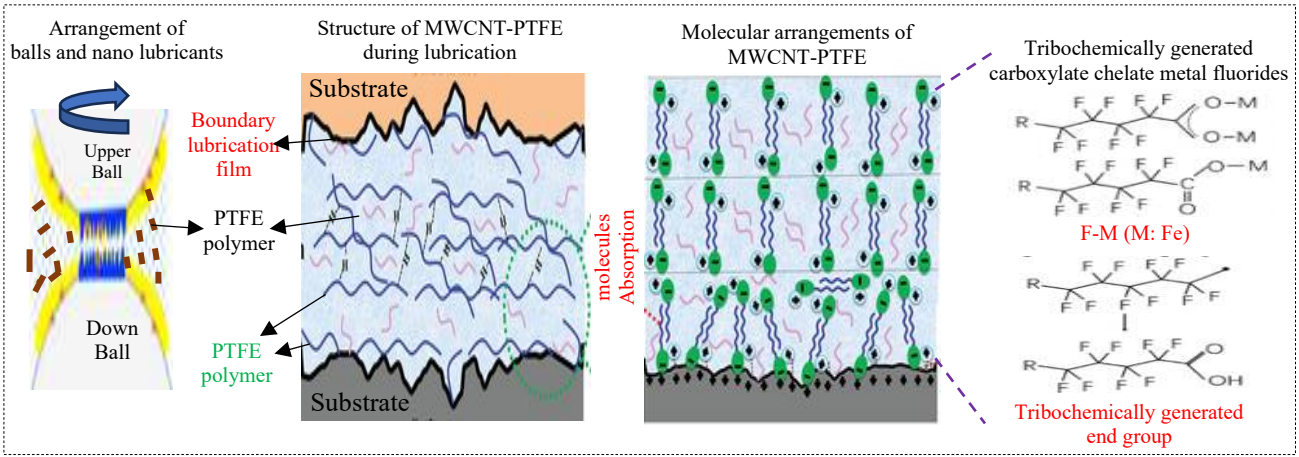


Fig. 10: Model mechanisms and tribo-film reactions towards tribo-pair wear shields for MWCNT/PTFE lubrication.

4. Conclusion

In this study, the tribological characteristics of base jatropha oil under sliding test conditions were investigated in relation to varying concentrations of MWCNT and PTFE nanoparticles. The following conclusions were drawn from the findings:

- The study found that adding specific additives raised the lubricant's VI and viscosity in viscometric tests, but this effect was more pronounced under PTFE. Using FT-IR analysis, the formulation confirmed the presence of functional groups required for lubrication, such as carbonyl, alkene, and aliphatic CH_2 and CH_3 groups.

- The sliding speed and operating load of the system have a significant impact on the nanofluid tribological properties of MWCNT and PTFE particles. PTFE offered good COF results with three distinct loads (40 kg, 60 kg, 80 kg, and 100 kg) operating at 80 rpm, however MWCNT produced greater wear resistance than base jatropha oil. All of the tested lubricants, however, performed better than the base jatropha when the load was increased to 80 kg with an operating speed of 80 kg; however, 0.4 wt.% PTFE (49.77 %) and 1 wt.% MWCNT (40.08 %) produced the best results in terms of COF and wear mitigation, respectively.

- The synergistic effect of MWCNTs and PTFE additives greatly decreased the friction coefficient and wear impact. The optimum results were shown by 0.8 wt.% MWCNTs + 0.4 wt.% PTFE (G), out of all the concentrations evaluated during the additives concentration combined testing. Under 100 kg, the highest performance was similarly observed at an operating speed of 1000 rpm. When compared to the base lubricant utilized, the combination of the additives reduced COF by 55.11 % and wear by 44.43 %%. This demonstrates that wear resistance performs better than coefficient of friction

- After the lubrication operations, the lubricated surface with 0.8 wt.%MWCNTs and 0.4 wt.% PTF4 (G) smoothed to the surface of the base lubricant, which was thought to be essential in lowering asperity-induced direct contact during operation. Complex tribo-chemical reactions took place as a result of the BJO's inclusion of MWCNTs and PTFE additives during the lubrication. Little elements of P, S, O, and Fe were found under EDS analysis on the steel substrate, along with elements of many carbon constituents. Owing to the tribo-film's strength in supporting significant loads during operation, the tribological performance was enhanced in terms of lowering wear and friction as well as load carrying capacity. An further test using a 3 D AFM machine revealed that the wear depth produced by the new lubricant 0.8 wt.% MWCNTs and 0.4 wt.% PTF4 (G) was less than that of the BJO lubricated surface, and as a result, it was suggested for industrial lubrication.

Declarations
Clinical trial number: not applicable.′

Data Availability
Data used are incorporated in the work

Competing interests
No competing interests.

Funding
Supported by Ministry of Higher Education Malaysia through the Fundamental Research Grant Scheme (FRGS) FRGS/1/2024/TK09/UMP/01/1, and Universiti Malaysia Pahang Al-Sultan Abdullah (UMPSA) under reference Grant RDU240110.

Authors' contributions

ACO proposed, conducted the review/writings; KK, supervisory/fund; SCM, edited; MFG, edited the manuscript; WSWH, reviewed the drafted manuscript; AA, reviewed. All authors cross-checked and approved before submission of the final manuscript.

Acknowledgement
The authors would like to express their gratitude to every member of Centre for Research in Advanced Fluid & Processes Universiti Malaysia Pahang Al-Sultan Abdullah (UMPSA), for the contributions in this work.

Reference

[1] J. Luo, M. Liu, and L. Ma, "Origin of friction and the new frictionless technology—Superlubricity: Advancements and future outlook," *Nano Energy*, vol. 86, p. 106092, Aug. 2021, doi: 10.1016/J.NANOEN.2021.106092.

[2] J. Luo and X. Zhou, "Superlubricitive engineering—Future industry nearly getting rid of wear and frictional energy consumption," *Friction 2019 8:4*, vol. 8, no. 4, pp. 643–665, Jun. 2020, doi: 10.1007/S40544-020-0393-0.

[3] Y. Zhang, Z. Shi, G. Zhang, X. Ren, and H. Xu, "Tribological Behavior of Cu-10Pb-10Sn/Steel Bimetals under Different Loads and Speeds: Dry, Kerosene, and Oil Lubrication Conditions," *Journal of Materials Engineering and Performance 2025 35:2*, vol. 35, no. 2, pp. 1171–1183, Oct. 2025, doi: 10.1007/s11665-025-11620-9.

[4] A. P. Singh, R. K. Dwivedi, A. Suhane, P. K. Chaurasiya, P. K. Jain, and K. Sachan, "Tribological performance of CuO nanoparticle-enhanced lubricants on AISI 52100 steel surfaces," *Industrial Lubrication and Tribology*, vol. 78, no. 1, pp. 115–122, Aug. 2025, doi: 10.1108/ILT-05-2025-0246.

[5] S. Salem, H. Abuzied, W. M. Sadek, K. Sakr, and T. Elmeligy, “Experimental evaluation of tribological behavior in engine lubricants with trace additions of CuO and TiO_2 nanoparticles,” *Journal of Engineering and Applied Science 2025 72:1*, vol. 72, no. 1, pp. 266-, Dec. 2025, doi: 10.1186/S44147-025-00855-X.

[6] J. Zhang *et al.*, “MoS2Lubricating Film Meets Supramolecular Gel: A Novel Composite Lubricating System for Space Applications,” *ACS Appl. Mater. Interfaces*, vol. 13, no. 48, pp. 58036–58047, Dec. 2021, doi: 10.1021/ACSAMI.1C20182.

[7] P. Jiao *et al.*, “Tribological properties of MoS2 nanosheets solid lubricant planted on TiO2 nanotube array bed,” *ElsevierP Jiao, H Li, G Zu, P Li, J Wu, J WangTribology International, 2018•Elsevier*, Accessed: Feb. 18, 2026. [Online]. Available: https://www.sciencedirect.com/science/article/pii/S0301679X18301956

[8] S. R. Beyanagari and J. Kandasamy, “Tribological performance evaluation of h-BN nanoparticle reinforced AA 7075 and as-cast AA7075 using Taguchi and genetic algorithm,” *Surf. Topogr.*, vol. 9, no. 4, p. 045009, Oct. 2021, doi: 10.1088/2051-672X/ac2795.

[9] A. C. Opia, M. F. Bin Abdollah, S. C. Mamah, M. A. Hamid, S. Syahrullail, and H. Amiruddin, “Comparison on Tribological Responsiveness of Jatropha Lubricant Modified with H-BN on AISI E-52100 Steel and 6061 Aluminum Alloy Materials,” *Society of Petroleum Engineers - SPE Nigeria Annual International Conference and Exhibition, NAIC 2025*, Aug. 2025, doi: 10.2118/228627-MS.

[10] M. K. Gupta and J. Bijwe, “A complex interdependence of dispersant in nano-suspensions with varying amount of graphite particles on its stability and tribological performance,” *Tribol. Int.*, vol. 142, Feb. 2020, doi: 10.1016/j.triboint.2019.105968.

[11] L. Wu, L. Gu, and R. Jian, “Lubrication mechanism of graphene nanoplates as oil additives for ceramics/steel sliding components,” *Ceram. Int.*, vol. 47, no. 12, pp. 16935–16942, Jun. 2021, doi: 10.1016/J.CERAMINT.2021.02.266.

[12] J. Sun and S. Du, “Application of graphene derivatives and their nanocomposites in tribology and lubrication: A review,” *RSC Adv.*, vol. 9, no. 69, pp. 40642–40661, 2019, doi: 10.1039/c9ra05679c.

[13] A. C. Opia *et al.*, “Lubricity effectiveness of bio-lubricant modified with multi-wall carbon nanotube and organic polymer,” *Wear*, vol. 528–529, Sep. 2023, doi: 10.1016/j.wear.2023.204974.

[14] A. C. Opia *et al.*, “Effect of Surfactants on the Tribological Behavior of Organic Carbon Nanotubes Particles Additive under Boundary Lubrication Conditions,” *Tribology Online*, vol. 17, no. 1, pp. 19–31, Feb. 2022, doi: 10.2474/trol.17.19.

[15] P. Nie, C. Min, H. J. Song, X. Chen, Z. Zhang, and K. Zhao, “Preparation and tribological properties of polyimide/carboxyl-functionalized multi-walled carbon nanotube nanocomposite films under seawater lubrication,”*Tribology Letters, 2015•Springer*, vol. 58, no. 1, pp. 1–12, 2015, doi: 10.1007/S11249-015-0476-7.

[16] C. Wu, Y. Wu, H. Zhao, S. Li, J. Ni, and X. Li, “Influence of hardness of nanoparticle additive in PTFE solid lubricant on tribological properties of GCr15 steel with bionic texture,” *Tribol. Int.*, vol. 189, Nov. 2023, doi: 10.1016/J.TRIBOINT.2023.108915.

[17] M. K. Dubey, J. Bijwe, and S. S. V. Ramakumar, “Nano-PTFE: New entrant as a very promising EP additive,” *Tribol. Int.*, vol. 87, pp. 121–131, 2015, doi: 10.1016/J.TRIBOINT.2015.01.026.

[18] Y. Liu *et al.*, “Novel concept of nano-additive design: PTFE@ silica Janus nanoparticles for water lubrication,” *SpringerY Liu, H He, M Yang, R Zhang, S Yu, T Yang, W Wang, F LiangFriction, 2024•Springer*, vol. 12, no. 2, pp. 258–270, Feb. 2024, doi: 10.1007/S40544-023-0749-3.

[19] A. I. Ali *et al.*, “Investigation on lubricity effectiveness Ficus carica lubricant modified with PTFE and TBHQ as additives for steel-steel contact application,” *Tribol. Int.*, vol. 194, Jun. 2024, doi: 10.1016/J.TRIBOINT.2024.109489.

[20] V. Saini, J. Bijwe, S. Seth, and S. S. V. Ramakumar, “Interfacial interaction of PTFE sub-micron particles in oil with steel surfaces as excellent extreme-pressure additive,” *J. Mol. Liq.*, vol. 325, Mar. 2021, doi: 10.1016/J.MOLLIQ.2020.115238.

[21] A. Opia, M. Hamid, … S. S.-M. T., and undefined 2021, “Biomass as a potential source of sustainable fuel, chemical and tribological materials–Overview,” *Materials Today: Proceedings, 2021•Elsevier*, Accessed: Jul. 09, 2026: https://www.sciencedirect.com/science/article/pii/S2214785320326602

[22] F. Li, X. He, A. Srishti, S. Song, “Water hyacinth for energy and environmental applications: A review,” *Bioresource Technology, 2021•Elsevier*, Accessed: Jul. 09, 2026. [Online]. Available: https://www.sciencedirect.com/science/article/pii/S0960852421001486

[23] C. Min, Z. He, D. Liu, K. Zhang, “Urea modified fluorinated carbon nanotubes: unique self-dispersed characteristic in water and high tribological performance as water-based lubricant additives,”*Journal of Chemistry, 2019•pubs.rsc.org*, Accessed: Jul. 09, 2026: https://pubs.rsc.org/en/content/articlehtml/2019/nj/c9nj03099a

[24] I. Popa, G. Gillies, G. Papastavrou, and M. Borkovec, “Attractive and repulsive electrostatic forces between positively charged latex particles in the presence of anionic linear polyelectrolytes,”*The Journal of Physical Chemistry B, 2010•ACS Publications*, vol. 114, no. 9, pp. 3170–3177, Mar. 2010, doi: 10.1021/JP911482A.

[25] Q. Lu *et al.*, “Enhanced lubricity and anti-wear performance of zwitterionic polymer-modified N-enriched porous carbon nanosheets as water-based lubricant additive,” *ElsevierQ Lu, T Zhang, B He, F Xu, S Liu, Q Ye, F ZhouTribology International, 2022•Elsevier*, Accessed: Jul. 09, 2026. [Online]. Available: https://www.sciencedirect.com/science/article/pii/S0301679X21005697

[26] J. Guegan, M. Southby, and H. Spikes, “Friction modifier additives, synergies and antagonisms,” *SpringerJ Guegan, M Southby, H SpikesTribology Letters, 2019•Springer*, vol. 67, no. 3, Sep. 2019, doi: 10.1007/S11249-019-1198-Z.

[27] B. Zhao and L. Zhu, “Mixed polymer brush-grafted particles: a new class of environmentally responsive nanostructured materials,” *ACS PublicationsB Zhao, L ZhuMacromolecules, 2009•ACS Publications*, vol. 42, no. 24, pp. 9369–9383, Dec. 2009, doi: 10.1021/MA902042X.

[28] A. Hamnas and U. G. Panicker, “Sustainable bio-lubricant blends from mustard oil and castor oil: physico-chemical, thermal, rheological, and tribological characterizations for eco-friendly alternatives to commercial engine oil,” *Biomass Convers. Biorefin.*, vol. 15, no. 3, pp. 4607–4616, Feb. 2025, doi: 10.1007/s13399-024-05330-w.

[29] M. Z. Bahrom *et al.*, “Tribological Performance of Hexagonal Boron Nitride (h-BN) Nanoparticle Additives in Multigrade Motorcycle Engine Oils,” *Journal of Advanced Research in Micro and Nano Engineering*, vol. 29, no. 1, pp. 91–103, Mar. 2025, doi: 10.37934/armne.29.1.91103.

[30] A. I. Ali *et al.*, “Experimental analysis of tribological performance of base ficus carica vegetable oil with different polymers as additives using four ball tribometer,” *Mater. Today Proc.*, vol. 110, no. C, pp. 9–14, 2022, doi: 10.1016/j.matpr.2023.08.039.

[31] R. Kozdrach, P. Radulski, R. Kozdrach, and P. Radulski, “Analysis of the MSD, ICF Function, G’ and G” Modulus and Raman and FTIR Spectroscopy Spectra to Explain Changes in the Microstructure of Vegetable Lubricants,” *Lubricants 2025, Vol. 13,* vol. 13, no. 9, Sep. 2025, doi: 10.3390/LUBRICANTS13090416.

[32] A. C. Opia *et al.*, “Lubricity effectiveness of bio-lubricant modified with multi-wall carbon nanotube and organic polymer,” *Wear*, vol. 528–529, p. 204974, Sep. 2023, doi: 10.1016/J.WEAR.2023.204974.

[33] A. C. Opia *et al.*, “Tribological behavior of organic formulated anti-wear additive under high frequency reciprocating rig and unidirectional orientations: Particles transport behavior and film formation mechanism,” *Tribol. Int.*, vol. 167, p. 107415, Mar. 2022, doi: 10.1016/J.TRIBOINT.2021.107415.

[34] L. Liu, L. Wang, S. Sun, Y. Zhang, C. Zhang, and S. Zhang, “Study on the synergistic lubrication mechanism between sulfur- phosphorus-free ionic liquid-type organic molybdenum and ZDDP,” *Tribol. Int.*, vol. 195, Jul. 2024, doi: 10.1016/J.TRIBOINT.2024.109663.

[35] A. I. Ali *et al.*, “Assessment on oxidative stability and tribological response of Ficus carica Oil, enhanced with TBHQ and EVA additives,” *Tribol. Int.*, vol. 209, no. 2, p. 110735, Sep. 2025, doi: 10.1016/j.triboint.2025.110735.

[36] H. Wang, Z. Shao, K. Shen, B. Bateer, F. Ren, and X. Qi, “Super Hydrophobic UHMWPE/PTFE/PVA Composites with Low Friction: Preparation and Wear Mechanism,” *Polymers 2025, Vol. 17,* vol. 17, no. 12, Jun. 2025, doi: 10.3390/POLYM17121664.

[37] Y. Luo *et al.*, “Lubrication mechanism of PTFE on iron-based tribopairs in liquid oxygen under various loads: A reactive molecular dynamics study,” *Tribol. Int.*, vol. 221, p. 112021, Sep. 2026, doi: 10.1016/J.TRIBOINT.2026.112021.

[38] W. Sun, J. Ye, Q. Song, Y. Feng, and X. Liu, “Ultralow friction PTFE/PEEK heterolayer: A new solid lubrication approach toward simplicity,” *Friction 2023 12:1*, vol. 12, no. 1, pp. 120–135, Jun. 2023, doi: 10.1007/S40544-023-0747-9.

[39] Q. Zheng *et al.*, “Superlubricity of PTFE triggered by green ionic liquids,” *Appl. Surf. Sci.*, vol. 614, p. 156241, Mar. 2023, doi: 10.1016/J.APSUSC.2022.156241.

[40] M. Marian, M. Bartz, S. Wartzack, and A. Rosenkranz, “Non-Dimensional Groups, Film Thickness Equations and Correction Factors for Elastohydrodynamic Lubrication: A Review,” *Lubricants 2020, Vol. 8,* vol. 8, no. 10, pp. 1–20, Oct. 2020, doi: 10.3390/LUBRICANTS8100095.

[41] A. A. Lubrecht, C. H. Venner, and F. Colin, “Film thickness calculation in elasto-hydrodynamic lubricated line and elliptical contacts: The Dowson, Higginson, Hamrock contribution,” *Proceedings of the Institution of Mechanical Engineers, Part J: Journal of Engineering Tribology*, vol. 223, no. 3, pp. 511–515, May 2009, doi: 10.1243/13506501JET508;WGROUP:STRING:PUBLICATION.

[42] G. Boidi, J. C. João, F. J. Profito, and A. Rosenkranz, “Ti3C2Tx MXene Nanosheets as Lubricant Additives to Lower Friction under High Loads, Sliding Ratios, and Elevated Temperatures,” *ACS Appl. Nano Mater.*, vol. 6, no. 1, pp. 729–737, Jan. 2022, doi: 10.1021/ACSANM.2C05033.

[43] C. Du *et al.*, “Probing the lubricative behaviors of a high MXene-content epoxy-based composite under dry sliding,” *ElsevierCF Du, Z Wang, X Wang, X Zhao, J Gao, Y Xue, Y Jiang, H Yu, Q YeTribology International, 2022•Elsevier*, Accessed: Mar. 20, 2026. [Online]. Available: https://www.sciencedirect.com/science/article/pii/S0301679X2100462X